Progress in Reaction Kinetics and Mechanism

COMMUNICATION

Open Access

https://doi.org/10.48130/prkm-0026-0016

*Progress in Reaction Kinetics and Mechanism* **2026**, 51: e020

# A method for determining parameters of the modified random pore model (MRPM) for biomass char-$CO_2$ gasification

Lijuan Zhang[1], Mengzhao Liu[2*], Yi Wu[3] and Ping Geng[1*]

[1] *School of Agricultural Engineering and Food Science, Shandong Research Center of Engineering & Technology for Clean Energy, Shandong University of Technology, Zibo 255000, China*

[2] *Analysis and Testing Center, Shandong University of Technology, Zibo 255000, China*

[3] *Beijing Vocational College of Labour and Social Security, Beijing 100000, China*

* Correspondence: liumengzhao107@163.com (Liu M); gengping@sdut.edu.cn (Geng P)

## Abstract

The kinetic modeling of biomass char-$CO_2$ gasification is of great significance for the development of gasification technologies, process analysis, and equipment design optimization. Compared with other models, the modified random pore model (MRPM) exhibits distinct advantages in describing the kinetic mechanism of biomass gasification. However, methods for determining the model parameters of MRPM have not yet been reported in the literature, which increases the difficulty of applying MRPM to biomass gasification studies. This paper proposes a systematic method for solving the kinetic parameters of MRPM. Two biomass chars with distinctly different properties, namely coffee grounds char (CGC) and bamboo char (BBC), were used to validate the proposed method. The results show that the MRPM constructed using the proposed method can accurately fit the *r-X* and *X-t* curves of both CGC and BBC. The parameter-solving method for MRPM presented in this work is verified to be effective and reliable.

**Keywords:** Biomass, Gasification, MRPM

**Citation:** Zhang L, Liu M, Wu Y, Geng P. 2026. A method for determining parameters of the modified random pore model (MRPM) for biomass char-$CO_2$ gasification. *Progress in Reaction Kinetics and Mechanism* 51: e020 https://doi.org/10.48130/prkm-0026-0016

## Introduction

Kinetic modeling of char-$CO_2$ gasification is a cornerstone for optimizing gasifier design and improving reaction process efficiency. To characterize the evolution of sample properties during gasification, a suite of kinetic models has been proposed, including the volume-reaction model (VM), shrinking core model (SCM), integrated model (ICM), random pore model (RPM), and modified random pore model (MRPM)[1–3]. Coal and biomass feedstocks exhibit significant differences in physical and chemical properties[4,5], and these material characteristic variations lead to distinct applicability of different kinetic models[6–8]. Consequently, different biomass types often require tailored kinetic descriptions to achieve accurate modeling.

Extensive research has been conducted on kinetic modeling of various biomass feedstocks using different mechanism models. Zhang et al.[9] established kinetic models for 14 biomass types, including woody and herbaceous fuels with marked variations in alkali and alkaline earth metal (AAEM, i.e., K, Ca, Na) contents. Their findings indicated that only MRPM could adequately describe the gasification behavior of five biomass samples with unique reactivity profiles. Gupta et al.[5] compared the performance of VM, SCM, RPM, and MRPM in simulating $CO_2$ gasification of six AAEM-enriched biomass chars, and concluded that MRPM yielded the most accurate characterization of gasification kinetics. The high AAEM content in biomass introduces complexity to its gasification behavior and elevates the challenge of kinetic modeling[10–12]. As a result, the more mechanistically comprehensive MRPM has emerged as a preferred choice for establishing biomass gasification kinetic mechanisms.

Accurate determination of model parameters is the foundation of reliable kinetic modeling. For simplified models like VM and SCM, the rate constant can be directly derived by fitting experimental reaction rate or conversion curves[13]. For the conventional RPM, the structural parameter $\Psi$ is usually pre-determined, after which the rate constant is fitted[14,15]. Two main approaches are used to estimate $\Psi$: empirical estimation[16] and numerical fitting[17]. MRPM features a more complex mathematical structure, introducing two additional dimensionless correction parameters ($p$ and $c$) alongside $\Psi$, which further complicates the modeling process[18]. However, no detailed modeling procedure or parameter-solving method for MRPM has been reported.

Given MRPM's status as one of the most promising models for biomass gasification kinetics, developing an effective and universal parameter estimation framework is of great practical significance. This work presents a simple, robust, and universally applicable stepwise method for determining the complete set of MRPM kinetic parameters.

## Materials and methods

### *Materials and equipment*

Two representative biomass feedstocks were selected for this study: coffee grounds and bamboo. Coffee grounds are a low-ash, calcium-rich seed-derived biomass, whereas bamboo is a potassium-rich herbaceous biomass. Approximately 20 g of raw material (0.2–0.25 mm in particle size) was heated to 1,203 K in a fixed-bed reactor with $N_2$ flow and maintained at that temperature for 10 min to produce biomass chars. The obtained char was subsequently ground and sieved, with the 0.063–0.075 mm particle size fraction collected for subsequent gasification experiments. The properties of the CGC and BBC are shown in Table 1. The coffee grounds char and

https://doi.org/10.48130/prkm-0026-0016

**Table 1.** Properties of CGC and BBC.

| | Proximate analysis (wt%, db) | | | Ultimate analysis (wt%, db) | | | | Ash analysis (wt%) | | | | | |
|---|---|---|---|---|---|---|---|---|---|---|---|---|---|
| | A | V | FC | C | H | N | (O+S)[a] | $Al_2O_3$ | $SiO_2$ | $K_2O$ | CaO | $Fe_2O_3$ | Others |
| CGC | 2.1 | 15.9 | 82 | 77.1 | 1.4 | 3.1 | 16.3 | 5.2 | 3.7 | 1.9 | 40.5 | 0 | 48.7 |
| BBC | 14.4 | 6.9 | 78.7 | 75.5 | 1.3 | 0.3 | 8.5 | 0.2 | 26.7 | 59.8 | 1.4 | 0.5 | 11.4 |

a: By difference.

bamboo char were labeled CGC and BBC, respectively. Sample loading was performed using a flat alumina disc (FAD) without sidewalls. Samples were coded as S-C-M, where S = sample type, C = crucible type, and M = sample mass (e.g., CGC-FAD-1).

## Gasification experiments

Samples were heated at 50 K/min to the target temperature under 200 mL/min $N_2$ and held isothermally for 10 min. Isothermal $CO_2$ gasification was initiated by switching to a $CO_2$-containing gas stream and continued until the mass stabilized. The $CO_2$ partial pressure was adjusted by mixing $CO_2$ and $N_2$ at atmospheric pressure.

All gasification experiments were repeated twice, and the average values were reported. The relative standard deviations of the calculated kinetic parameters ($K$, $\Psi$, $c$, $p$) were ± 5% in CGC and ± 8% in BBC, indicating good reproducibility.

Char conversion ($X$) and isothermal reactivity ($r$, $min^{-1}$) of the char during the isothermal gasification are determined from Eqs. (1) and (2), respectively.

$$X = \frac{m_0 - m_t}{m_0 - m_g} \tag{1}$$

$$r = \frac{d_X}{d_t} \tag{2}$$

where, $m_0$ represents the original mass of the sample at the onset of gasification, $m_t$ denotes the instantaneous mass at time $t$ during gasification, $t$; and $m_e$ stands for the final sample mass upon completion of gasification, equivalent to the ash mass.

## Kinetic mechanism model of gasification reaction

The differential of the RPM and MRPM can be expressed as Eqs. (3) and (4). $c$ and $p$ are dimensionless parameters. Because of the complexity of MRPM, it is difficult to obtain the analytic solution of its integral form. Figure 1a–f shows the $r$-$X$ curve of MRPM with different model parameters. With the constant adjustment of $\Psi$, $p$, and $c$, the position of the peak reaction rate changes obviously. Moreover, the $r$-$X$ curve shape is more abundant, which further expands the application scope of the model.

$$\frac{d_X}{d_t} = K(1-X)\sqrt{1-\psi\ln(1-X)} \tag{3}$$

$$\frac{d_X}{d_t} = K(1-X)\sqrt{1-\psi\ln(1-X)}(1+(cX)^p) \tag{4}$$

# Results and discussion

Based on the trajectory characteristics of the $r$-$X$ curve of CGC and BBC in Fig. 2, the changes in $r$-$X$ curves of CGC and BBC are more complicated, presenting a trend of an increase before a decrease, and the peak position and variation trend of reaction rate are obviously different.

In the proposed parameter determination method, the rate constant $K$ of the MRPM is solved first, followed by the structural parameter $\Psi$, and the correction parameters $c$ and $p$. By taking the limit of the MRPM kinetic function as conversion approaches zero, Eq. (5) is derived. It indicates that the model rate constant $K$ corresponds to the initial reaction rate at $X$ = 0. However, directly using the

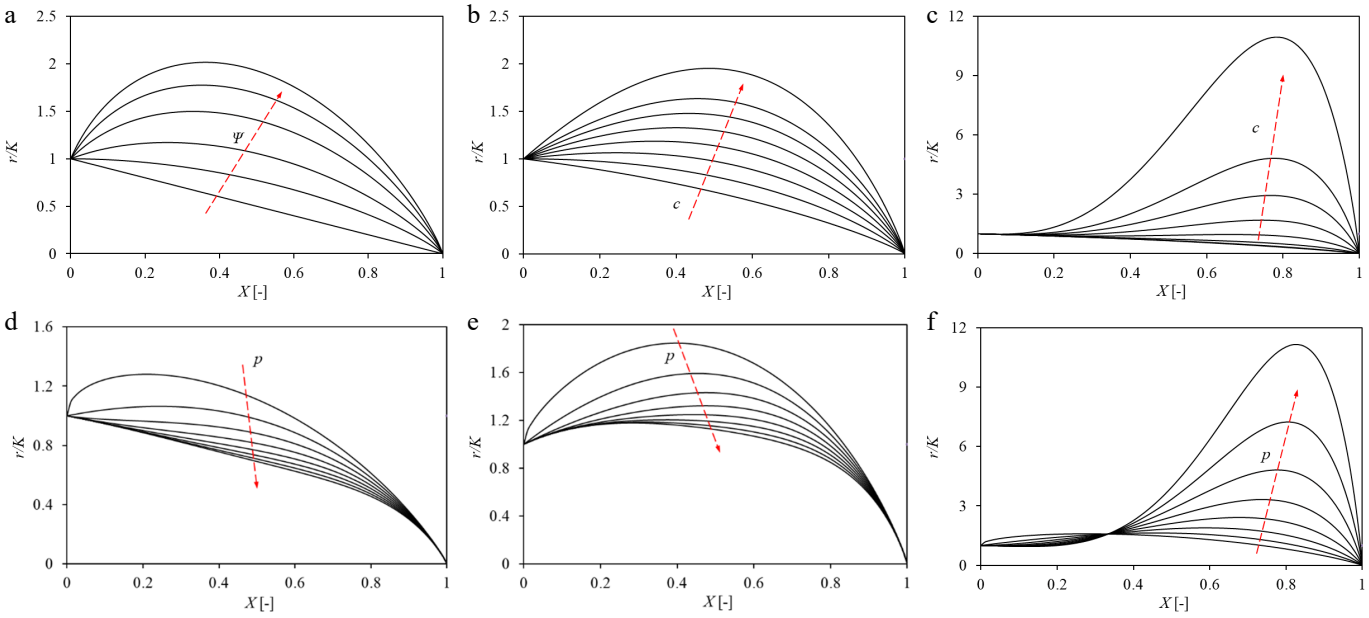


**Fig. 1** The $r$-$X$ curves of MRPM. (a) MRPM, $\Psi$: 0–20, $p$, $c$ = 0. (b) MRPM, $\Psi$ = 1, $p$ = 1, $c$: 0–4. (c) MRPM, $\Psi$ = 1, $p$ = 3, $c$: 0-4. (d) MRPM, $\Psi$ = 1, $c$ = 1, $p$: 0.5–4. (e) MRPM, $\Psi$ = 5, $c$ = 1, $p$: 0.5–4. (f) MRPM, $\Psi$ = 1, $c$ = 3, $p$: 0.5–4.

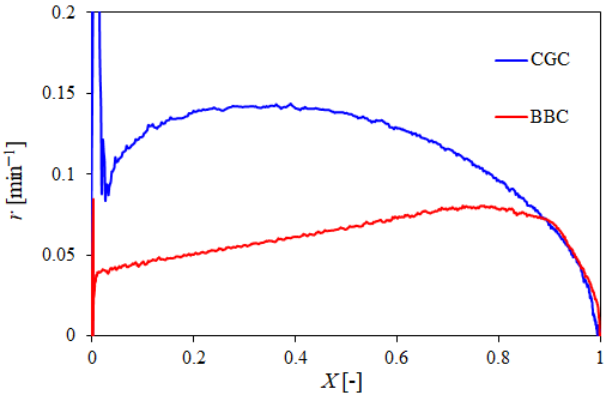


**Fig. 2** The *r*-*X* curves of CGC and BBC.

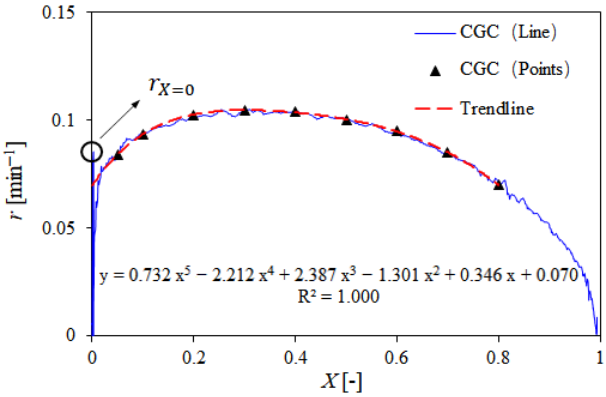


**Fig. 3** Determination of reaction rate at $X = 0$.

experimental reaction rate at $X = 0$ is unreliable, as it is affected by gas switching hysteresis, transient flow disturbances, and pressure fluctuations at the onset of gasification[19]. To obtain an accurate and physically meaningful initial reaction rate, reaction rates within the conversion range of $X = 0.1$–$0.8$ were fitted with a smooth function, and the value at $X = 0$ was then extrapolated. Taking CGC as an example, the procedure for determining the initial reaction rate is illustrated in Fig. 3. Using this method, the rate constants $K$ for CGC-FAD-1 and BBC-FAD-1 under different temperatures and $CO_2$ partial pressures were obtained, as listed in Table 2.

$$\frac{d_X}{d_t}|_{X\to 0} = \lim_{X\to 0}\left[K(1-X)\sqrt{1-\psi(\ln(1-X))}(1+(cX)^p)\right] = K \qquad (5)$$

As MRPM is derived as an extension of the conventional RPM, the stable $\Psi$ at low conversion rates ($X < 0.3$) represents the intrinsic pore structure unaffected by AAEM catalysis at higher conversions; therefore, $\Psi$ is first reliably estimated using the RPM form (as a fixed MRPM parameter), after which the scaling parameters $c$ and $p$ (which primarily influence medium-to-high conversions, $X > 0.5$) are introduced. With the rate constant $K$ already obtained, $\Psi$ becomes the only unknown parameter in the RPM equation. Therefore, $\Psi$ can be calculated by substituting the experimental reaction rate at a given conversion $X$ into the RPM expression. The calculated $\Psi$ values for CGC-FAD-1 and BBC-FAD-1 at various conversion points are presented in Table 3.

It can be seen from Table 3 that for CGC-FAD-1, the calculated $\Psi$ remains relatively stable at approximately $10.9 \pm 0.3$ when $X < 0.5$, but increases abruptly at higher conversions. This suggests that the conventional RPM with a constant $\Psi = 10.9 \pm 0.3$ cannot reasonably describe the gasification reaction rate of CGC-FAD-1 at $X > 0.5$. For BBC-FAD-1, $\Psi$ is nearly constant at around 8.3 in the low conversion range ( $X < 0.3$) and rises sharply afterward, indicating that RPM fails to capture the reactivity evolution of BBC-FAD-1 at $X > 0.3$.

To further verify this limitation, the *r*-*X* and *X*-*t* curves of CGC-FAD-1 and BBC-FAD-1 were fitted using RPM, and the results are displayed in Fig. 4. As observed, the fitting accuracy of RPM deteriorates noticeably for CGC-FAD-1 at $X > 0.5$ and becomes unsatisfactory for BBC-FAD-1 even at $X > 0.3$. These fitting results are highly consistent with the variation trends of $\Psi$ shown in Table 3, confirming the inherent limitation of RPM in describing the mid-to-high conversion behavior of biomass chars.

To improve the fitting performance at medium and high conversions, the additional correction parameters $c$ and $p$ in MRPM were introduced and determined. In this step, the stable $\Psi$ values in the low-conversion stage were adopted: 10.9 for CGC-FAD-1 and 8.3 for BBC-FAD-1. With $K$ and $\Psi$ fixed, only $c$ and $p$ remain unknown in Eq. (4). By substituting the experimental reaction rates at no fewer than two conversion points within the poorly fitted region into the MRPM differential equation, the values of $c$ and $p$ can be solved analytically. The obtained parameters for CGC-FAD-1 and BBC-FAD-1 under different conditions are listed in Table 4.

**Table 2.** The model rate constants of CGC and BBC.

| | T (K) | P (MPa) | | | |
|---|---|---|---|---|---|
| | | 0.025 | 0.05 | 0.075 | 0.1 |
| CGC-FAD-1 | 1,173 | 0.070 | 0.093 | 0.112 | 0.131 |
| | 1,123 | 0.025 | 0.032 | – | – |
| BBC-FAD-1 | 1,173 | 0.020 | 0.027 | 0.033 | 0.037 |
| | 1,123 | 0.008 | 0.011 | – | – |

**Table 3.** The model parameter $\Psi$ of CGC-FAD-1 and BBC-FAD-1.

| | T (K) | P (MPa) | *X* | | | | | | |
|---|---|---|---|---|---|---|---|---|---|
| | | | 0.2 | 0.3 | 0.4 | 0.5 | 0.6 | 0.7 | 0.8 |
| CGC-FAD-1 | 1,173 | 0.025 | 11.0 | 11.1 | 10.9 | 10.8 | 11.2 | 12.0 | 14.6 |
| | | 0.05 | 10.9 | 10.6 | 10.6 | 10.9 | 11.4 | 13.6 | 15.5 |
| | | 0.075 | 10.8 | 10.7 | 10.6 | 10.8 | 11.5 | 13.2 | 15.6 |
| | | 0.1 | 10.6 | 10.7 | 10.8 | 10.7 | 11.0 | 12.2 | 15.0 |
| | 1,123 | 0.025 | 11.2 | 11.0 | 10.9 | 11.1 | 11.5 | 12.6 | 14.5 |
| | | 0.05 | 10.8 | 11.1 | 11.2 | 11.0 | 11.4 | 12.2 | 14.6 |
| BBC-FAD-1 | 1,173 | 0.025 | 8.2 | 10.0 | 12.3 | 15.6 | 20.8 | 29.8 | 46.2 |
| | | 0.05 | 8.3 | 10.2 | 12.6 | 16.3 | 22.6 | 33.5 | 53.7 |
| | | 0.075 | 8.3 | 10.1 | 12.7 | 16.7 | 23.7 | 36.7 | 60.9 |
| | | 0.1 | 8.2 | 9.8 | 12.5 | 16.8 | 24.6 | 39.4 | 67.8 |
| | 1,123 | 0.025 | 8.3 | 9.5 | 11.0 | 15.1 | 21.7 | 34.2 | 62.5 |
| | | 0.05 | 8.2 | 9.0 | 11.4 | 15.7 | 22.7 | 36.9 | 64.1 |

https://doi.org/10.48130/prkm-0026-0016

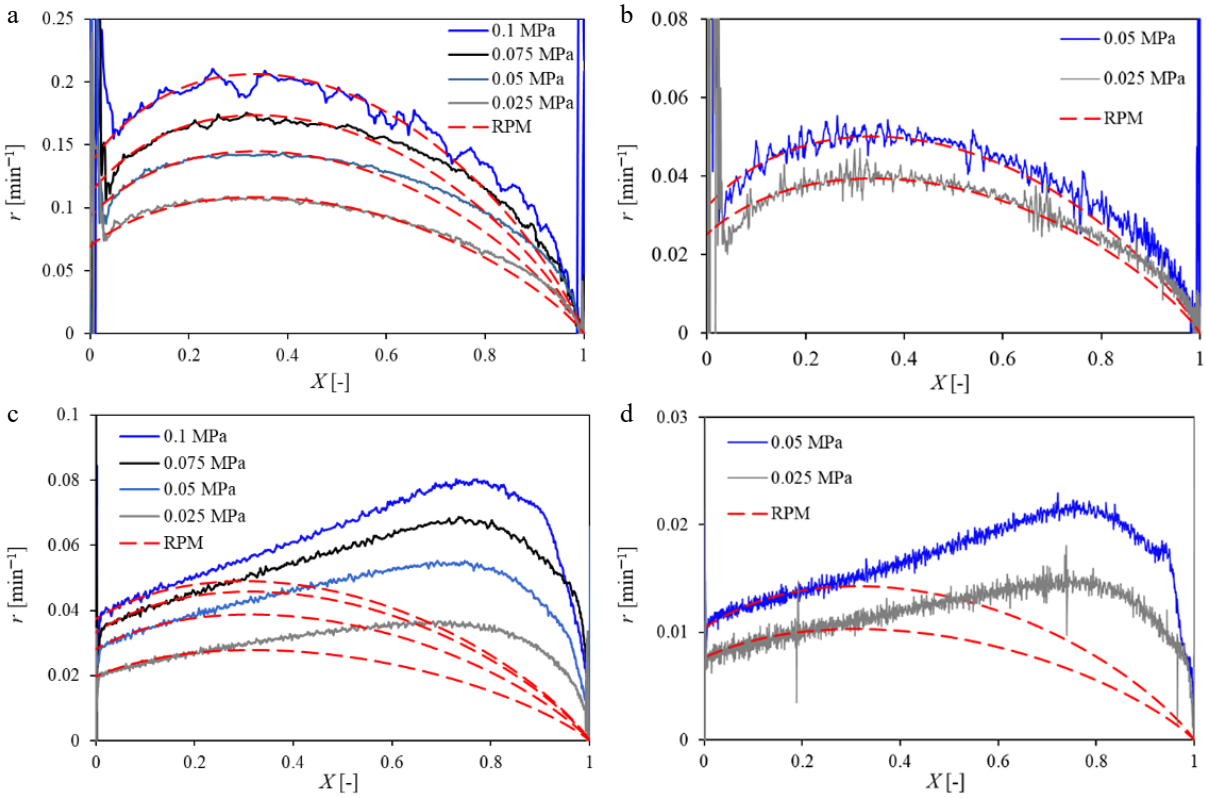


**Fig. 4** The model-fitting results of RPM to CGC-FAD-1 and BBC-FAD-1. (a) CGC-FAD-1 (1,173 K). (b) CGC-FAD-1 (1,123 K). (c) BBC-FAD-1 (1,173 K). (d) BBC-FAD-1 (1,123 K).

**Table 4.** The model parameters of CGC-FAD-1 and BBC-FAD-1.

| | T (K) | P (MPa) | *p* | *c* |
|---|---|---|---|---|
| CGC-FAD-1 | 1,173 | 0.025 | 6.4 | 0.9 |
| | | 0.05 | 6.5 | 1.0 |
| | | 0.075 | 6.3 | 1.0 |
| | | 0.1 | 6.4 | 1.0 |
| | 1,123 | 0.025 | 6.3 | 0.9 |
| | | 0.05 | 6.5 | 1.0 |
| BBC-FAD-1 | 1,173 | 0.025 | 3.2 | 1.4 |
| | | 0.05 | 3.2 | 1.3 |
| | | 0.075 | 3.4 | 1.5 |
| | | 0.1 | 3.3 | 1.5 |
| | 1,123 | 0.025 | 3.3 | 1.4 |
| | | 0.05 | 3.4 | 1.4 |

To validate the reliability and effectiveness of the proposed parameter-solving method, all the obtained kinetic parameters (*K*, *Ψ*, *c*, and *p*) were substituted into the MRPM equation to fit the full-range *r*-*X* and *X*-*t* curves of CGC-FAD-1 and BBC-FAD-1. The fitting results are presented in Fig. 5. As shown in Fig. 5, the MRPM established using the proposed method achieves excellent agreement with experimental data for CGC-FAD-1 throughout the entire conversion range. For BBC-FAD-1, the model also provides satisfactory fitting quality up to $X < 0.9$. These results clearly demonstrate that the stepwise parameter determination method is reliable and feasible. By introducing the correction parameters *c* and *p*, MRPM effectively overcomes the shortcomings of RPM and enables an accurate description of the $CO_2$ gasification kinetics of biomass chars with distinct physicochemical properties. Specifically, they mathematically compensate for the complex structural changes that occur during the medium to high conversion stages, such as pore coalescence, carbon matrix collapse, and the continuously increasing diffusion resistance caused by ash layers, which cannot be captured by the traditional RPM framework.

## Conclusions

A systematic and feasible method for determining the kinetic parameters of the modified random pore model during biomass char-$CO_2$ gasification was proposed in this work. Using two typical biomass chars with distinct physicochemical properties as validation samples, the model parameters, including the rate constant *K*, structural parameter *Ψ*, and correction parameters *c* and *p*, were successfully solved step by step.

The results demonstrate that the MRPM established via the proposed method can accurately fit the full-range reactivity-conversion (*r*-*X*) and conversion-time (*X*-*t*) curves of both CGC and BBC. Compared with the conventional RPM, which fails to accurately describe the gasification behavior at medium and high conversions, the parameter-optimized MRPM exhibits significantly improved fitting accuracy and broader applicability to different biomass chars. This method is established for the biomass char-$CO_2$ gasification system and is also well applicable to biomass char with high ash and high AAEM content.

The proposed parameter-solving procedure is straightforward, reliable, and does not require complex iterative algorithms or numerical optimization. For kinetic modeling of the $CO_2$ gasification of the two biomass chars examined in this work (coffee ground char and bamboo char), it serves as a simple and effective framework—rather than a universally applicable one. While extrapolation

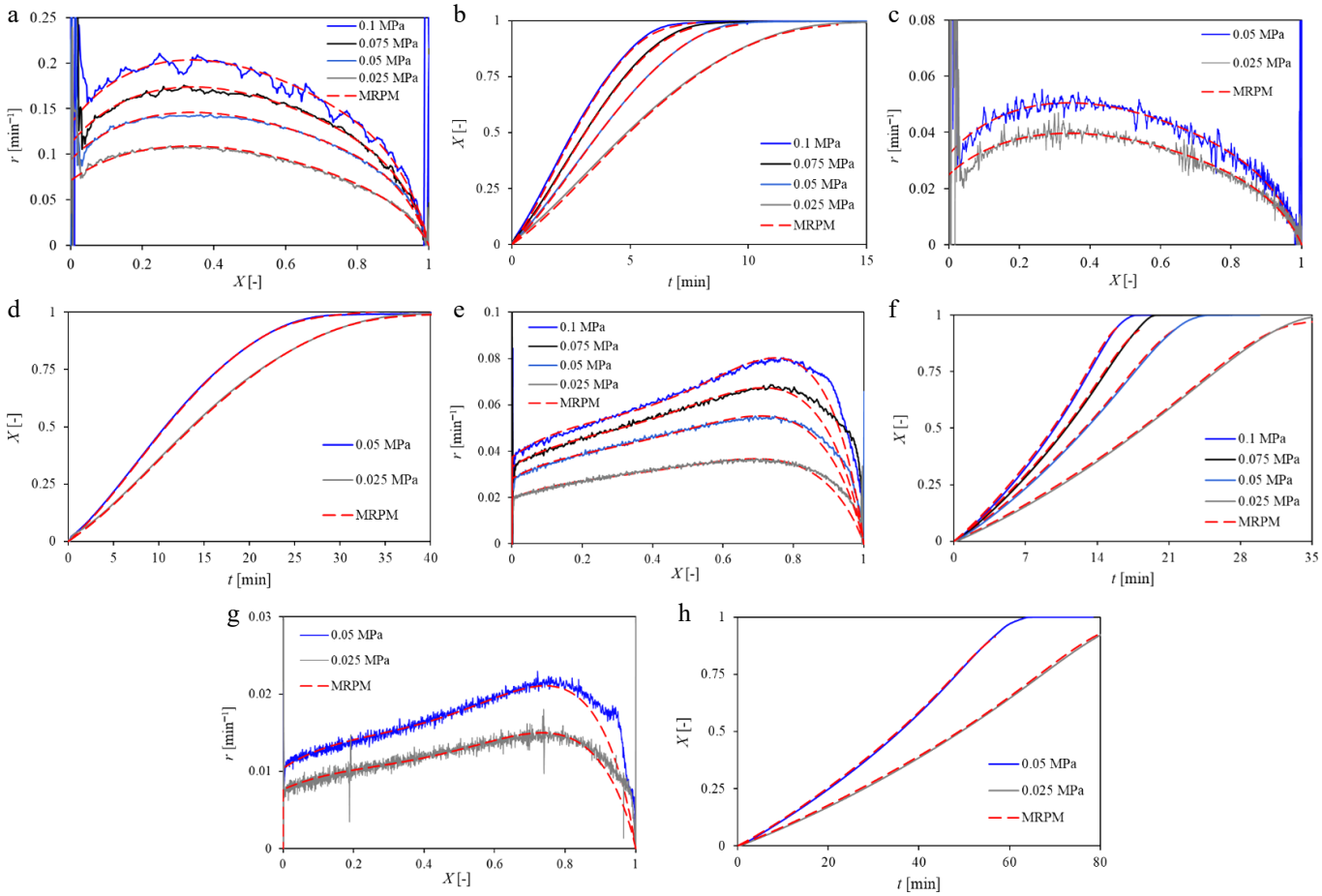


**Fig. 5** The model-fitting results of MRPM to CGC-FAD-1 and BBC-FAD-1. (a) *r*-*X* (CGC-FAD-1, 1,173 K). (b) *X*-*t* (CGC-FAD-1, 1,173 K). (c) *r*-*X* (CGC-FAD-1, 1,123 K). (d) *X*-*t* (CGC-FAD-1, 1,123 K). (e) *r*-*X* (BBC-FAD-1, 1,173 K). (f) *X*-*t* (BBC-FAD-1, 1,173 K). (g) *r*-*X* (BBC-FAD-1, 1,123 K). (h) *X*-*t* (BBC-FAD-1, 1,123 K).

to other char-gas reactions and other biomass types would require further experimental verification, the procedure demonstrates clear promise and could, after appropriate validation, become a useful tool for kinetic mechanism research, reactor simulation, and process design of gasification systems.

## Author contributions

The authors confirm their contributions to the paper as follows: study conception and design, project administration: Liu M, Geng P; investigation and resources: Wu Y; data curation and draft manuscript preparation: Zhang L; supervision: Geng P. All authors reviewed the results and approved the final version of the manuscript.

## Data availability

The datasets generated during and/or analyzed during the current study are available from the corresponding author upon reasonable request.

## Acknowledgments

The authors acknowledge the financial support provided by the Natural Science Foundation of Shandong Province. (Grant No. ZR2024QB415).

## Conflict of interest

The authors declare that they have no known competing financial interests or personal relationships that could have appeared to influence the work reported in this paper.

## Dates

Received 30 March 2026; Revised 23 April 2026; Accepted 15 May 2026; Published online 3 July 2026

## References

[1] Dang H, Xu R, Zhang J, Wang M, Zhang J. 2025. Interaction mechanism and kinetic modeling of anthracite and power plant biomass waste during $CO_2$ co-gasification process. *Energy* 325:136115

[2] Cao X, Bu C, Han Q, Zhao X, Piao G. 2024. Kinetic analysis and model evaluation for steam co-gasification of coal-biomass blended chars using macro-TGA. *Fuel Processing Technology* 266:108151

[3] Ding L, Wang S, Li X, Bai T, Qiu Z, et al. 2024. Experimental and kinetic study of pressurized $CO_2$ gasification of biomass chars. *Chemical Engineering Research and Design* 212:349–361

[4] Wei R, Ren L, Liu L. 2026. Gasification reactivity and kinetic simulation of anthracite/biomass chars and co-pyrolysis chars. *Renewable Energy* 256:123916

[5] Gupta A, Thengane SK, Mahajani S. 2018. $CO_2$ gasification of char from lignocellulosic garden waste: experimental and kinetic study. *Bioresource Technology* 263:180–191

https://doi.org/10.48130/prkm-0026-0016

[6] Iwaszenko S, Howaniec N, Smoliński A. 2019. Determination of random pore model parameters for underground coal gasification simulation. *Energy* 166:972–978
[7] Kudva IK, Shinde SG, Pandit K, Fan LS. 2026. Kinetic insights into biomass char gasification for chemical looping reactor design. *Chemical Engineering and Processing - Process Intensification* 219:110617
[8] Cortazar M, Lopez G, Alvarez J, Arregi A, Amutio M, et al. 2020. Experimental study and modeling of biomass char gasification kinetics in a novel thermogravimetric flow reactor. *Chemical Engineering Journal* 396:125200
[9] Zhang Y, Ashizawa M, Kajitani S, Miura K. 2008. Proposal of a semi-empirical kinetic model to reconcile with gasification reactivity profiles of biomass chars. *Fuel* 87:475–481
[10] Grasa G, Martínez I, Murillo R. 2024. Gasification kinetics of chars from diverse residues under suitable conditions for the Sorption Enhanced Gasification process. *Biomass and Bioenergy* 180:107000
[11] Felix CB, Chen WH, Ubando AT, Park YK, Lin KYA, et al. 2022. A comprehensive review of thermogravimetric analysis in lignocellulosic and algal biomass gasification. *Chemical Engineering Journal* 445:136730
[12] Chew JJ, Soh M, Sunarso J, Yong ST, Doshi V, et al. 2020. Isothermal kinetic study of $CO_2$ gasification of torrefied oil palm biomass. *Biomass and Bioenergy* 134:105487
[13] Morin M, Pécate S, Hémati M. 2018. Kinetic study of biomass char combustion in a low temperature fluidized bed reactor. *Chemical Engineering Journal* 331:265–277
[14] Betancur M, Arenas CN, Martínez JD, Navarro MV, Murillo R. 2020. $CO_2$ gasification of char derived from waste tire pyrolysis: Kinetic models comparison. *Fuel* 273:117745
[15] Parandin MS, Ale Ebrahim H, Norouzi HR. 2024. Towards random pore model for non-catalytic gas-solid reactions. *Renewable and Sustainable Energy Reviews* 202:114731
[16] González-Vázquez MP, García R, Gil MV, Pevida C, Rubiera F. 2018. Unconventional biomass fuels for steam gasification: kinetic analysis and effect of ash composition on reactivity. *Energy* 155:426–437
[17] Gil MV, Fermoso J, Pevida C, Pis JJ, Rubiera F. 2010. Intrinsic char reactivity of plastic waste (PET) during $CO_2$ gasification. *Fuel Processing Technology* 91:1776–1781
[18] Kramb J, DeMartini N, Perander M, Moilanen A, Konttinen J. 2016. Modeling of the catalytic effects of potassium and calcium on spruce wood gasification in $CO_2$. *Fuel Processing Technology* 148:50–59
[19] Gomez A, Silbermann R, Mahinpey N. 2014. A comprehensive experimental procedure for $CO_2$ coal gasification: is there really a maximum reaction rate? *Applied Energy* 124:73–81